Laakmann *et al.*
Cell Communication and Signaling (2023) 21:111
https://doi.org/10.1186/s12964-023-01131-2

Cell Communication and Signaling

RESEARCH

Open Access

Bacterial extracellular vesicles repress the vascular protective factor RNase1 in human lung endothelial cells

Katrin Laakmann[1], Jorina Mona Eckersberg[1], Moritz Hapke[1], Marie Wiegand[1], Jeff Bierwagen[1], Isabell Beinborn[1], Christian Preußer[2], Elke Pogge von Strandmann[2], Thomas Heimerl[3], Bernd Schmeck[1,3,4,5,6] and Anna Lena Jung[1,4*]

Abstract

Background Sepsis is one of the leading causes of death worldwide and characterized by blood stream infections associated with a dysregulated host response and endothelial cell (EC) dysfunction. Ribonuclease 1 (RNase1) acts as a protective factor of vascular homeostasis and is known to be repressed by massive and persistent inflammation, associated to the development of vascular pathologies. Bacterial extracellular vesicles (bEVs) are released upon infection and may interact with ECs to mediate EC barrier dysfunction. Here, we investigated the impact of bEVs of sepsis-related pathogens on human EC RNase1 regulation.

Methods bEVs from sepsis-associated bacteria were isolated via ultrafiltration and size exclusion chromatography and used for stimulation of human lung microvascular ECs combined with and without signaling pathway inhibitor treatments.

Results bEVs from *Escherichia coli*, *Klebsiella pneumoniae* and *Salmonella enterica* serovar Typhimurium significantly reduced RNase1 mRNA and protein expression and activated ECs, while TLR2-inducing bEVs from *Streptococcus pneumoniae* did not. These effects were mediated via LPS-dependent TLR4 signaling cascades as they could be blocked by Polymyxin B. Additionally, LPS-free *ClearColi*™ had no impact on RNase1. Further characterization of TLR4 downstream pathways involving NF-κB and p38, as well as JAK1/STAT1 signaling, revealed that RNase1 mRNA regulation is mediated via a p38-dependent mechanism.

Conclusion Blood stream bEVs from gram-negative, sepsis-associated bacteria reduce the vascular protective factor RNase1, opening new avenues for therapeutical intervention of EC dysfunction via promotion of RNase1 integrity.

Keywords Sepsis, OMV, Ribonuclease 1, Endothelium, Inflammation, TLR4, Polymyxin B, p38

*Correspondence:
Anna Lena Jung
anna.jung@uni-marburg.de
Full list of author information is available at the end of the article

Introduction

Sepsis is one of the leading causes of death worldwide with approximately 50 million cases per year [1]. Development and progression of sepsis is mainly caused by bacterial infections of the lung, urinary tract, skin and intestine [1–5]. Accordingly, frequent pathogens like gram-positive *Streptococcus pneumoniae* (*Sp*) as well as gram-negative, increasingly antibiotic-resistant *Enterobacteriaceae* like *Escherichia coli* (*Ec*), *Klebsiella pneumoniae* (*Kp*) or *Salmonella enterica* (*Sal*) are of major interest [6, 7]. Exemplarily, severe lung infections cause a breakdown of the alveolar membrane and enable the invasion of bacterial pathogens into the bloodstream [3, 7]. These systemic infections provoke an imbalanced immune response of the host that finally ends up in vascular barrier breakdown, multi-organ failure and death [8, 9]. In this regard, sepsis progression is characterized by excessive production of pro-inflammatory cytokines and a pro-coagulant state of the vasculature that further promotes endothelial cell (EC) dysfunction [2, 3, 5].

Besides classical inflammatory factors like cytokines or chemokines, extracellular vesicles (EVs) play an essential role during infection and inflammation as novel mediators of intercellular communication [10]. EVs are small, nano- to micrometer sized, spherical membrane enclosed structures that can be released by eukaryotic host cells as well as bacteria (bEVs; [11]). bEVs from bacteria can further be separated into two classes, outer membrane vesicles (OMVs) that are secreted by gram-negative bacteria and membrane vesicles (MVs) that are secreted by gram-positive bacteria [11–13]. In respect to pneumonia, various studies describe a wide range of bEV functions in host–pathogen interactions (reviewed in: [11]) and an additional impact of bEVs in blood stream infection is currently under consideration. Thereby, bEVs can either be released by circulating pathogens, but are also capable of reaching distant organs independently of the secreting bacteria [14], where they fulfill an essential role in progression of sepsis-associated dysfunction of the endothelium [15–20]. The pathogen-EC interaction is primarily regulated by bacterial immune agonists like lipopolysaccharide (LPS) or lipoprotein that are also associated to the bEV surface [21]. Those known pattern-recognition receptor ligands can further induce inflammation and intracellular signaling in the endothelium, such as activation of Toll-like receptors (TLRs) that promote disruption of the EC barrier and immune function [16, 22]. Cell membrane-bound TLRs like TLR2 or TLR4 can sense bEVs and induce downstream signaling via the MyD88/IRAK-1 axis that is mediated by IRAK-1 degradation to further promote NF-κB translocation to the nucleus as well as p38 phosphorylation and translocation to activate associated gene expression. Additionally, TLR4 can also induce TRIF-dependent signaling upon endocytosis that promotes IRF3/7-mediated type I interferon (IFN) production and subsequent activation o the f type I IFN receptor (IFNAR) and the JAK/STAT pathway (Fig. S1) [23–25].

ECs function as a protective barrier to separate the blood from the surrounding tissue and act as regulators of vascular homeostasis [26–28]. Upon inflammation, ECs get activated, which is characterized for instance by secretion of pro- and antithrombotic factors as well as upregulation of pro-inflammatory mediators like adhesion molecules and cytokines (e.g., intercellular adhesion molecule 1 (ICAM-1), C-X-C motif chemokine ligand 8 (CXCL8), C-X-C motif chemokine ligand 10 (CXCL10)) [15, 26–29]. Thereby, massive and persistent inflammation can tremendously harm the homeostatic function of the endothelium and is involved in development of vascular dysfunctions such as sepsis-associated formation of micro-thrombosis or intravascular coagulation [15, 27].

Endothelial Ribonuclease 1 (RNase1) is known as an important vessel- and tissue-protective factor [30–33], countering the damage associated molecular pattern extracellular RNA (eRNA) to prevent excessive EC inflammation [34]. However, massive inflammation results in eRNA-induced EC inflammation and RNase1 repression, effected by massive amounts of pro-inflammatory mediators like tumor necrosis factor alpha (TNF-α) [34–36], that promotes EC dysfunction and development of vascular pathologies including thrombosis [30, 34, 37–41]. Besides these data, recent studies also investigated the role of the RNase1-eRNA system in sepsis suggesting a potential RNase1 repression during disease progression as well as a protective function of RNase1 during sepsis-associated tissue- and organ damage [42, 43]. Altogether, the current literature suggests a causal interaction between sepsis-associated EC dysfunction and RNase1 repression that is still insufficiently studied.

Here, we investigated the impact of bEVs from different sepsis-associated bacterial pathogens on the regulation of the vessel-protective factor RNase1 and the underlying signaling cascades in human lung ECs. In this study, we found that OMVs from the gram-negative bacteria *Escherichia coli*, *Klebsiella pneumoniae* and *Salmonella enterica* serovar Typhimurium repress endothelial RNase1 via an LPS-induced TLR4-IRAK-1 and p38-mediated mechanism to promote EC inflammation that favors development of endothelial dysfunction independent of the investigated donor bacteria.

Material and methods

Bacterial vesicle generation and isolation

Escherichia coli (#25922, *Ec*), *Klebsiella pneumoniae* (#700721/MGH78578, *Kp*), and *Salmonella enterica* serovar Typhimurium (#14028, *Sal*) were purchased from American Type Culture Collection (ATCC; Manassas, USA). *ClearColi*™ BL21 (*cC*) were obtained from BioCat GmbH (Heidelberg, Germany). *Streptococcus pneumoniae* (D39, *Sp*) were kindly provided by Sven Hammerschmidt (University Greifswald, Germany). *Ec*, *Kp* and *Sal* were cultivated on MacConkey agar plates, *cC* in LB with 1% NaCl and *Sp* on blood agar plates overnight at 37°C and 5% CO_2. Bacteria were then used for inoculation of liquid culture media (LB: *Ec*, *Kp, Sal*; LB + 1% NaCl: *cC*; THY: *Sp*) and grown until they reached the late exponential phase with shaking at 160 rpm and 37°C (MaxQ 6000, Thermo Fisher Scientific, Waltham, USA) excluding *Sp*, which were cultivated without shaking. To obtain a medium control for following stimulation experiments, LB medium and THY medium was handled in parallel to bacterial liquid cultures during vesicle preparation serving as medium controls without bacterial growth. Next, bacterial cultures, LB and THY media were centrifuged three times at 4,800 xg for 20 min at 4 °C (Multifuge X3R, Thermo Fisher Scientific) and residual bacteria were removed from the supernatant by using a 0.22 µm pore sterile filter unit. Bacterial vesicles and medium were further processed by ultrafiltration and size exclusion chromatography (UF-SEC) as follows: Bacterial/medium supernatants were concentrated using a 100 kDa molecular weight cut-off filter (Merck Millipore, Burlington, Sigma Aldrich, St. Lois, USA) to a final volume of 500 µl, which was further processed by size exclusion chromatography using the qEVoriginal/ 70 nm Gen 2 columns (IZON Science LTD, Lyon, France). Vesicle elution was proceeded using 0.1 µm filtered PBS and 24 SEC-fractions were collected (500 µl/fraction). Vesicle enriched fractions (7–12) were concentrated to a final volume between 200 and 400 µl using molecular weight cut-off filters (Merck Millipore) and particle concentration was determined by nano-flow cytometry (nanoFCM; NanoFCM Co., Ltd, Nottingham, UK). Equal amounts of vesicles per cell (multiplicity of vesicles of 1000; MOV_{1000}) were used for stimulation experiments. Each bacterial vesicle preparation was checked for contaminating bacteria by plating on blood agar plates. Vesicles were aliquoted and stored at -20°C as working stocks.

nanoFCM

nanoFCM measurements of bEV preparations to determine bEV concentration and size distribution were performed as previously described by Bierwagen et al. 2023 [44].

Transmission Electron Microscopy (TEM)

TEM was performed to validate intact vesicle structures as previously described by Bierwagen *et al.* 2023 [44].

Cell culture

Cells used in this study were cultivated in a humidified incubator at 37°C with 5% CO_2. Human microvascular lung endothelial cells (HULEC-5a) (CRL-3244™, ATCC) were cultured in human microvascular endothelial cell medium MCDB 131 (Gibco™, Thermo Fisher Scientific) supplemented with 10% fetal calf serum (Capricorn Scientific GmbH, Ebsdorfergrund, Germany), 1% penicillin and streptomycin (Gibco™, Thermo Fisher Scientific), 10 mM GlutaMax™ (Gibco®, Thermo Fisher Scientific), 10 ng/ml EGF (Merck Millipore, Sigma Aldrich) and 1 µg/ml hydrocortisone (Th. Geyer Ingredients GmbH & Co. KG, Höxter, Germany). Cells were cultured up to passage 20 for all experiments.

Stimulation of endothelial cells

Cells were seeded with $3.8*10^4$ cells/cm^2 overnight followed by stimulation for 16 or 24 h (mRNA expression and ELISA) or 0–180 min (Western Blot) as indicated: TNF-α (10 ng/ml) (R&D Systems, Inc., Minneapolis, USA), LPS from *Escherichia coli* O111:B4 (100 ng/ml) (cell culture grade, Sigma Aldrich), LPS from *Salmonella minnesota* R595 (100 ng/ml) (cell culture grade, Enzo Life Sciences, Lausen, Switzerland), IFN-ɣ (250 ng/ml) (Promo Cell, Heidelberg, Germany) or with vesicles from gram-negative bacteria (OMVs) from *Escherichia coli* (*Ec*OMV), *Klebsiella pneumoniae* (*Kp*OMV), *Salmonella enterica* serovar Typhimurium (*Sal*OMV), *Clear coli* (*cC*OMV) or MVs from gram-positive *Streptococcus pneumoniae* (*Sp*MV) with MOV_{1000}, respectively. For Polymyxin B treatment (PB; Merck Millipore), OMVs were preincubated for 1 h with the LPS neutralizing antibiotic PB (20 µg/ml) (Merck Millipore) followed by stimulation as indicated. For inhibitor experiments, HULEC-5a were pretreated for 1 h with the JAK1 inhibitor Ruxolitinib (5 µM; JAKi) (Biozol Diagnostics Vertrieb GmbH, Eching, Germany), the NF-κB inhibitor BAY11-7082 (5 µM; NF-κBi) or the p38 inhibitor SB202190 (10 µM; p38i) (Merck Millipore) prior to indicated stimulation. Dimethyl sulfoxide (DMSO, Carl Roth GmbH + Co. KG, Karlsruhe, Germany) served as solvent control.

Table 1 Primer sequences 5′➔3′

Primer	Forward	Reverse
CXCL8	ACTGAGAGTGATTGAGAG TGGAC	AACCCTCTGCACCCAGTTTTC
CXCL10	CTGCCATTCTGATTTGCTGCC	GATGCAGGTACAGCGTACAG
ICAM-1	CTCAGTCAGTGTGACCGC	CCTTCTGAGACCTCTGGC
RNase1	GCTGCAGATCCAGGCTTTTCT GGG	AATTTCTTGGCCCGGGATTC
RPS18	GCGGCGGAAAATAGCCTTTG	GATCACACGTTCCACCTCATC
TLR2	GGCCAGCAAATTACCTGTGTG	AGGCGGACATCCTGAACCT
TLR4	TGAGACCAGAAAGCTGGGAG	ACTCTGGATGGGGTTTCCTG

RNA isolation and quantitative reverse transcription PCR

Total RNA was isolated from HULEC-5a and cDNA was generated as described previously [36]. mRNA transcript expression of RNase1, CXCL8, ICAM-1, CXCL10, TLR2 and TLR4 was analyzed by quantitative reverse transcription PCR (qPCR) compared to RPS18 that served as internal control. Respective primer pairs are listed in Table 1 (Metabion international AG, Planegg/Steinkirchen, Germany). qPCR was performed using LUNA® Universal qPCR Master Mix (New England Biolabs, Ipswich, USA) and the QuantStudio™ System and QuantStudio™ Design & Analysis Software v1.3.1 (both Thermo Fisher Scientific) according to the manufacturer's instructions. The $2^{-\Delta\Delta ct}$ method was used for calculation of the fold-induction and qPCR results were normalized to the corresponding control cells [45].

LDH-assay

Cytotoxicity of HULEC-5a upon stimulation was determined via lactate dehydrogenase (LDH) release into supernatants compared to a total lysis (TL) representing 100% cell death using the Pierce™ LDH Cytotoxicity Assay Kit (Roche, Mannheim, Germany) according to the manufacturer's protocol. The absorbance was measured using the infinite F200Pro microplate reader (Tecan, Männedorf, Switzerland).

Protein isolation for Western Blot

HULEC-5a were seeded and stimulated as described before for 0–180 min as indicated. For isolation of total protein, cells were washed once with PBS and stored dry at -20°C until further processing. Cells were scraped and lysed in RIPA buffer (containing cOmplete™ mini protease inhibitor cocktail and PhosSTOP™, Merck Millipore) followed by sonication via ultrasound for 5 min (30 s on/off at 4°C). Samples were centrifuged for 20 min at 13,000 xg at 4 °C to remove cellular debris. For fractionation of cytosolic and nuclear proteins, HULEC-5a were seeded and stimulated as described above for 30 min. After stimulation, cells were scraped in 1 ml PBS and centrifuged at 240 xg at 4°C for 2 min to pellet cells. The supernatant was discarded, and the pellet was resuspended in fractionation buffer A (10 mM HEPES, pH 7.9, 10 mM KCl, 0.1 mM EDTA, 0.1 mM EGTA, supplemented with protease inhibitor as well as 0.5 mM DTT) and incubated for 15 min on ice. Cell disruption was additionally promoted by multiple aspirating of the suspension using a 26G needle and syringe, followed by centrifugation for 2 min at 4,400 xg at 4°C. For cytosolic protein isolation, the supernatant was centrifuged for additional 20 min at 20,000 xg at 4°C and stored at -80°C until further use. For nuclear protein isolation, the pellet was washed twice with fractionation buffer A and the nuclei containing pellet was resuspended in fractionation buffer B (20 mM HEPES, pH 7.9, 400 mM NaCl, 1 mM EDTA, 1 mM EGTA) and incubated for 30–60 min at 4 °C with shaking at 1,000 rpm. Samples were centrifuged for 20 min at 20,000 xg at 4°C and supernatants were stored at -80°C. Protein concentration of all samples was measured using the Pierce BCA protein assay kit according to the manufacturer's instructions (Thermo Fisher Scientific). Twenty-five microgram protein per sample and fifteen microgram for fractionation samples were loaded and separated on a 10% or 12.5% SDS PAGE gel (30 min at 80 V and subsequently ~ 120 min for total protein samples or ~ 180 min for fractionation samples at 120 V), respectively, followed by protein transfer and immobilization via wet blot procedure using a Perfect-Blue™ Tank Electro Blotter (VWR International, Radnor, USA) and Towbin buffer on 0.2 µm nitrocellulose membrane (GE Healthcare, Chicago, USA) for 1 h with 100 V at 4°C. Membranes were blocked and exposed to antibodies targeting IRAK-1 (4359S), phospho-p38 (Thr180/Tyr182) (9211S), p38 (9212S), STAT1 (D1K9Y, 14994S), phospho-STAT1 (Tyr701) (58D6, 9167S) (Cell Signaling, Cambridge, UK), p65 (F-6; sc-8008), Lamin A/C (H-110; sc-20681), α1c-Tubulin (MH-87, sc-134239) and β-actin (I-19, sc-1616) (Santa Cruz Biotechnology, Heidelberg, Germany) followed by incubation with respective secondary, HRP-conjugated antibodies: mouse anti-rabbit IgG-HRP (L27A9, 5127S; Cell Signaling) or anti-mouse m-IgGκ BP-HRP (sc-516102; Santa Cruz Biotechnology). Chemiluminescence was detected using Amersham™ ECL™ Prime Western Blotting Detection Reagent (RPN2236, cytiva, Merck Millipore) and visualized by the ADVANCED Fluorescence and ECL Imager (Intas Science Imaging Instruments, Germany).

ELISA

Supernatants of stimulated HULEC-5a were used for protein detection of CXCL8 and RNase1 via ELISA. CXCL8 ELISA was performed as recommended by

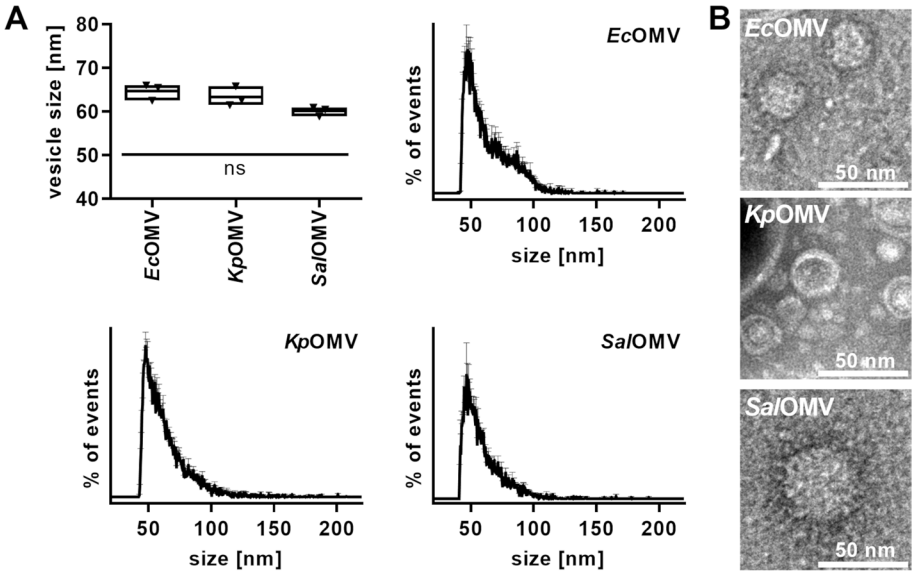

Fig. 1 Characterization of bacterial outer membrane vesicles. **A)** Mean size of SEC-purified OMVs from *Escherichia coli* (*Ec*OMV), *Klebsiella pneumoniae* (*Kp*OMVs) and *Salmonella enterica* serovar Typhimurium (*Sal*OMV) and their size distribution profile was determined by nanoFCM. $n = 3$, line at mean, One-way ANOVA with Tukey's multiple comparison test; ns: not significant. **B)** Vesicle shape and structure was validated by transmission electron microscopy (TEM). Scale bar: 50 nm

the manufacturer's protocol using the BD OptEIA™ Human IL-8 ELISA Set (555244, BD Biosciences, Franklin Lakes, USA). RNase1 ELISA was performed using the human Ribonuclease A Matched ELISA Antibody Pair Set (SEK13468, Sino Biological, Inc., Beijing, China) as recommended by the manufacturer's instructions. Detection of HRP-mediated signal was performed using BD OptEIA™ TMB Substrate Reagent Set (555214, BD Biosciences) and the absorbance was measured using the microplate reader infinite F200Pro (Tecan).

Statistical analyses

Statistical analyses were performed using GraphPad Prism Version 9.5.0 (730) (GraphPad Software, La Jolla, CA, USA). qPCR results are expressed as log2 transformed data with line at mean. ELISA results are expressed as linear data, line at mean. One-way or two-way ANOVA were performed as indicated with subsequent multiple comparison using recommended post-tests as indicated in the figure legend. Results were considered significant at $p \leq 0.05$, which is labelled with * or # in the figures.

Availability of data and materials

All data generated or analyzed during this study are included in this article and its supplementary file.

Results

Characterization of bacterial vesicles

To investigate the impact of bacterial vesicles from the sepsis-associated gram-negative pathogens *Escherichia coli* (*Ec*OMVs), *Klebsiella pneumoniae* (*Kp*OMVs) and *Salmonella enterica* serovar Typhimurium (*Sal*OMVs) as well as the gram-positive pathogen *Streptococcus pneumoniae* (*Sp*MVs) on endothelial RNase1, OMVs and MVs were isolated from liquid bacterial culture via UF-SEC (Fig. S2A). Particle concentration and size distribution of isolated vesicles was investigated by nanoFCM. No significant differences were observed between the different vesicle types showing mean sizes of approximately 60–70 nm as well as their size distribution profile, peaking at ~ 50 nm (Fig. 1A and Fig. S2B-D). Further characterization of isolated bacterial vesicles was performed by TEM imaging showing intact, spherical, membrane enclosed structures for all tested vesicle types (Fig. 1B).

OMVs from *Ec*, *Kp*, *Sal* repress RNase1 and activate the endothelium

To analyze the regulatory potential of OMVs and MVs on endothelial RNase1 and their impact on proinflammatory EC activation, HULEC-5a were exposed to TNF-α (10 ng/ml) as positive control [36], *Ec*OMVs, *Kp*OMVs, *Sal*OMVs and *Sp*MVs with MOV_{1000} or left untreated as control (Ctrl) for 16 and 24 h (Fig. 2, Figs. S3A and S4). UF-SEC

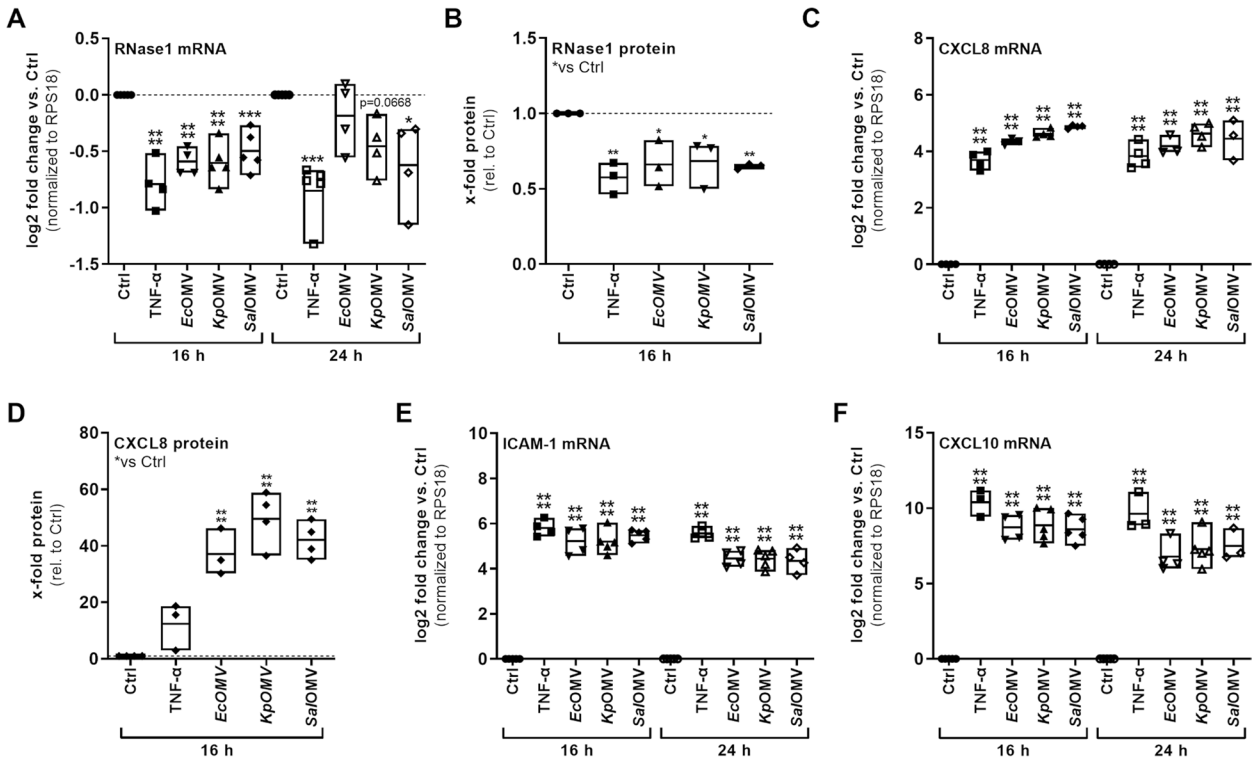

Fig. 2 OMVs repress endothelial RNase1 and induce proinflammatory EC activation. Human lung microvascular ECs (HULEC-5a) were stimulated for 16 h and 24 h with SEC-purified OMVs (MOV_{1000}) from *Ec*, *Kp* and *Sal* or TNF-α (10 ng/ml) or left untreated as control (Ctrl). mRNA expression of **A**) RNase1 **C**) CXCL8, **E**) ICAM-1 and **F**) CXCL10 was determined by qPCR, normalized to RPS18 and untreated cells (Ctrl). **B)** RNase1 and **D)** CXCL8 protein release in supernatants of 16 h stimulated HULEC-5a was measured by ELISA, depicted as x-fold protein relative to control (Ctrl). $n = 3–4$, line at mean, One-way ANOVA with Dunnett's multiple comparison test compared to respective Ctrl. $^{*}p < 0.05$, $^{**}p < 0.01$, $^{***}p < 0.001$, $^{****}p < 0.0001$

processed LB- or THY-medium served as medium control to assess potential effects of medium components on EC activation (Fig. S3B-C). Interestingly, RNase1 mRNA expression was significantly repressed by *Ec*OMVs, *Kp*OMVs, *Sal*OMVs treatment after 16 h, similar to stimulation with the RNase1-repressive cytokine TNF-α. This effect was less prominent at 24 h, although RNase1 mRNA remained suppressed (Fig. 2A). In contrast, no effect on RNase1 mRNA could be observed by stimulation with the gram-positive *Sp*MVs (Fig. S4A) as well as the LB and THY-medium controls (Fig. S3C). Similar to TNF-α, OMVs from *Ec*, *Kp*, *Sal* also repressed secretion of RNase1 protein measured by ELISA after 16 h stimulation (Fig. 2B), while *Sp*MV did not regulate RNase1 protein levels (Fig. S4B). Besides RNase1 regulation, all OMVs proinflammatory activated HULEC-5a after 16 and 24 h stimulation, as indicated by mRNA expression of CXCL8, ICAM-1 and CXCL10 (Fig. 2C, E–F), while this was not the case for *Sp*MV (Fig. S4C-E). Additionally, protein secretion of CXCL8 was also increased by OMV treatment (Fig. 2D). To ensure cell viability upon OMV and MV treatment, cytotoxicity of respective stimulants was obtained by LDH assay showing no significant increase in cytotoxicity upon exposure above a threshold of 30% cytotoxicity (Fig. S3A-B). Accordingly, OMVs from sepsis-associated gram-negative bacteria *Ec*, *Kp* and *Sal* specifically repressed endothelial RNase1 and activated human lung ECs, in contrast to gram-positive MVs from *Sp*. Based on these findings, further analysis focused on 16 h OMV treatment due to the observed significant RNase1 regulation in conjunction with a strong proinflammatory activation of the cells.

OMVs induce a TLR4-dependent signaling cascade in human ECs to repress RNase1

To understand the underlying mechanisms, we investigated the basal mRNA expression of specific TLRs that are needed to sense those bEV types on the cell surface: TLR2 for *Sp*MVs and TLR4 for all tested OMV types. Basal mRNA expression of TLR2 and TLR4 was investigated by qPCR. These data revealed substantial differences in TLR2 and TLR4 mRNA expression in HULEC-5a with low abundance for TLR2 compared to high abundance for TLR4 (Fig. S5). Thus, unresponsiveness of HULEC-5a to *Sp*MV might be associated to the low availability of TLR2, while abundant TLR4

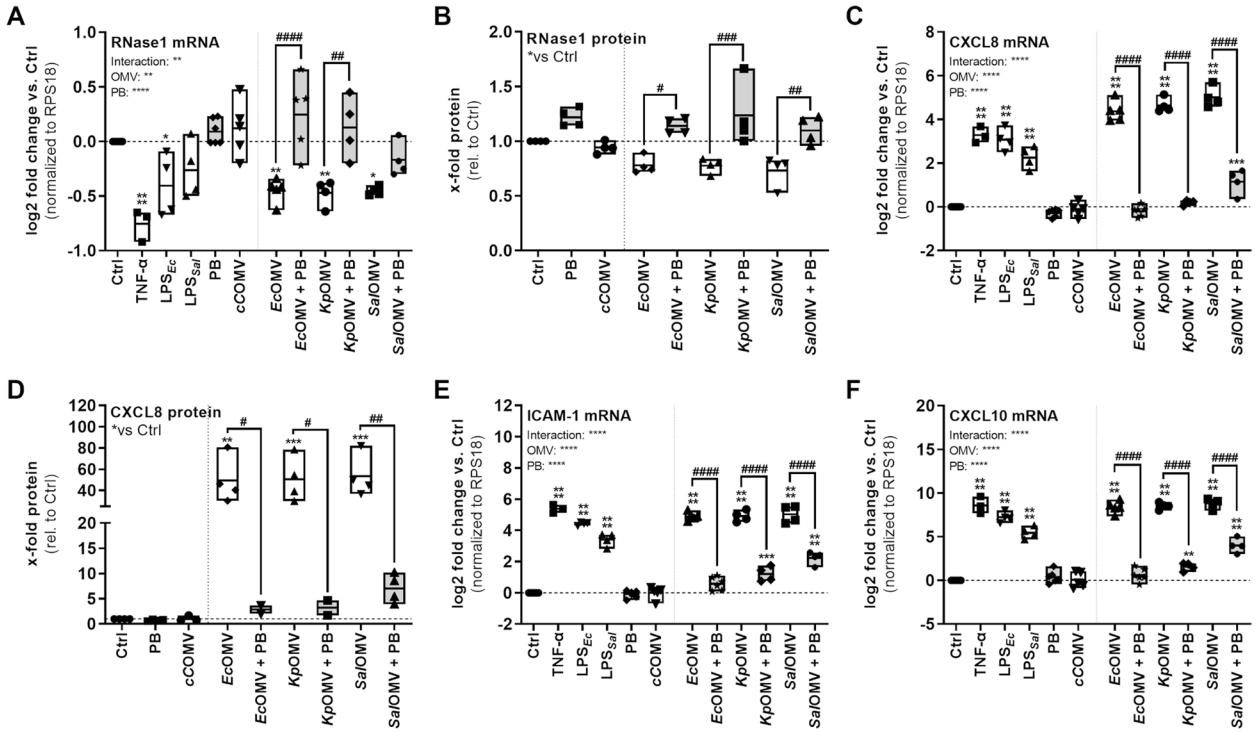

Fig. 3 OMVs repress endothelial RNase1 and induce proinflammatory EC activation in a TLR4-dependent manner. SEC-purified OMVs from *Ec*, *Kp* and *Sal* were pretreated for 1 h with 20 µg/ml Polymyxin B (PB) and further used for stimulation of HULEC-5a (MOV_{1000}) for 16 h, as well as TNF-α (10 ng/ml), LPS from *Ec* (LPS_{Ec}) or *Sal* (LPS_{Sal}) (100 ng/ml) or left untreated as control (Ctrl). mRNA expression of **A**) RNase1, **C**) CXCL8, **E**) ICAM-1 and **F**) CXCL10 was determined by qPCR, normalized to RPS18 and Ctrl. $n = 3–5$, line at mean, Two-way ANOVA with Tukey's multiple comparison test. **B)** RNase1 protein release and **D**) CXCL8 protein release from supernatants of 16 h stimulated HULEC-5a was measured by ELISA, depicted as x-fold protein relative to Ctrl. $n = 4$, line at mean, One-way ANOVA with Tukey's multiple comparison test. * compared to corresponding Ctrl, # as indicated. *$p < 0.05$, **$p < 0.01$, ***$p < 0.001$, ****$p < 0.0001$. #$p < 0.05$, ##$p < 0.01$, ####$p < 0.0001$

expression is a prerequisite for the responsiveness of these cells to *Ec*, *Kp* and *Sal* OMVs. To further unravel the intracellular signaling cascade that transmits OMV-mediated RNase1 repression, we addressed LPS that is exposed on the OMV surface as potent TLR4 agonist to induce proinflammatory signaling cascades via either the MyD88/IRAK-1 or the TRIF axis (Fig. S1) [23–25].

To block the potential LPS-mediated TLR4 induction by OMVs, the LPS neutralizing antibiotic Polymyxin B (PB) was used for further analysis (Fig. S1, Fig. 3) [46, 47]. *Ec*OMVs, *Kp*OMVs and *Sal*OMVs (MOV_{1000}) were pre-incubated with PB (20 µg/ml) for 1 h, prior to 16 h stimulation of HULEC-5a with untreated or PB-pretreated OMVs. For comparison purposes, cells were stimulated with LPS from *E. coli* (LPS_{Ec}) or *Salmonella* (LPS_{Sal}) (100 ng/ml), TNF-α (10 ng/ml) or left unstimulated (Ctrl). As an additional control, OMVs from endotoxin free *Clear coli* (*cC*OMVs), that carry a modified lipid A and have therefore a non-functional version of LPS, served as control as these bacteria are not able to elicit TLR4-mediated endotoxic responses [48]. *cC*OMVs were comparable in size to all other used OMVs and did not show any difference in their size distribution profile (Fig. S2B and D).

In accordance with previous results, TNF-α and OMVs significantly reduced RNase1 mRNA expression, while LPS from *Ec* and *Sal* only showed tendencies of RNase1 repression. Compared to that, stimulation with *cC*OMVs and the LPS-blocking agent PB did not influence RNase1 mRNA expression. Remarkably, stimulation of HULEC-5a with PB-pretreated OMVs (grey bars) significantly recovered RNase1 mRNA compared to the respective untreated OMVs (white bars) for *Ec*, *Kp* and *Sal*OMVs (Fig. 3A). Similar results were observed on protein level, where TNF-α and untreated OMVs, except *cC*OMVs, repressed RNase1 protein release which could be recovered by OMV-pretreatment with PB (Fig. 3B). In addition to RNase1 regulation, TNF-α, LPS_{Ec}, LPS_{Sal} and untreated OMVs, except *cC*OMVs, significantly induced proinflammatory EC activation as demonstrated by CXCL8 mRNA induction and protein release (Fig. 3C and D), ICAM-1 mRNA (Fig. 3E) and CXCL10 mRNA (Fig. 3F) compared to PB and Ctrl treatment. In addition, PB-pretreated OMVs were also not capable to induce a

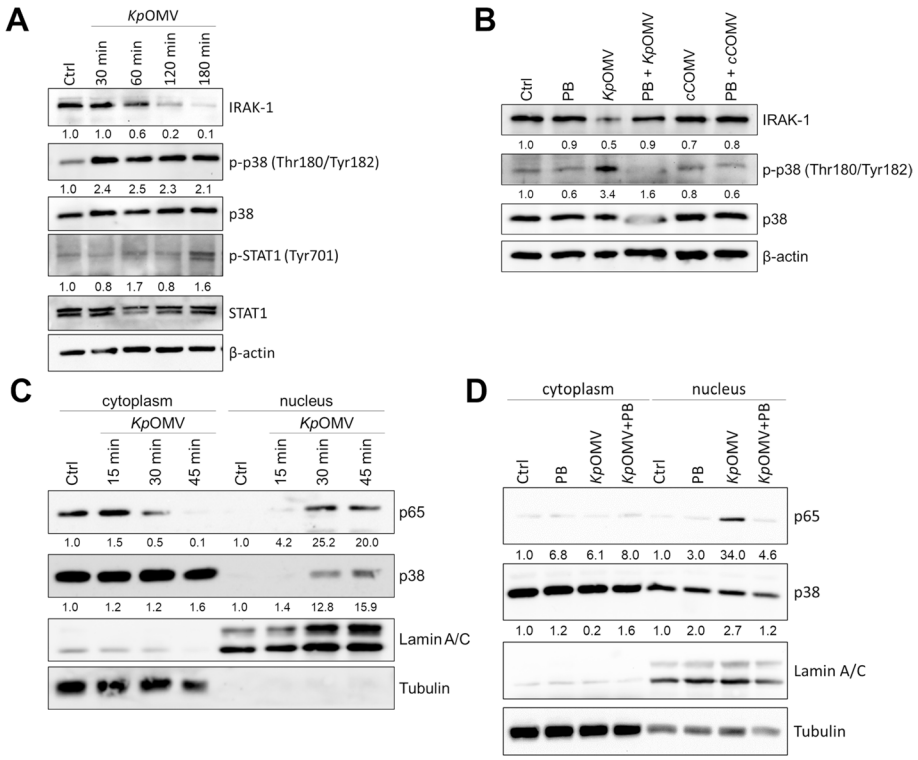

Fig. 4 OMVs induce proinflammatory signaling cascades in human lung ECs. **A)** Human lung microvascular ECs (HULEC-5a) were stimulated with SEC-purified *Kp*OMVs (MOV_{1000}) or left untreated as control (Ctrl). Expression and phosphorylation of IRAK-1, p38 and STAT1 after OMV exposure for up to 180 min were determined by Western Blot. β-actin served as a loading control. **B)** HULEC-5a were stimulated for 180 min with *Kp* or *c*COMVs (MOV_{1000}) alone or in combination with PB (20 µg/ml) or left untreated for Ctrl. Expression and phosphorylation of IRAK-1 and p38 was determined by Western Blot. β-actin served as a loading control. **C)** HULEC-5a were incubated with *Kp*OMV for up to 45 min or **D**) incubated with *Kp*OMV for 30 min with or without 1 h pretreatment with PB (20 µg/ml). Samples were fractionated into cytosolic and nuclear proteins and analyzed by Western Blot for p65 and p38. Tubulin served as a cytoplasmic loading control, while Lamin A/C served as a nuclear loading control. One representative result of three biological independent replicates is shown

strong proinflammatory response. Additionally, none of the stimulations induced significant changes in cytotoxicity (Fig. S3D).

To further validate the previous observations on protein level, activation of the TLR4-associated intracellular signaling molecules (Fig. S1) in *Kp*OMV-stimulated ECs (MOV_{1000} for 0–180 min) was analyzed. Degradation of IRAK-1, phosphorylation of p38 (at threonine 180 and tyrosine 182) and phosphorylation of STAT1 (at tyrosine 701) were investigated by Western Blot along with the loading control β-actin (Fig. 4A). IRAK-1 degradation started at approximately 60 min after OMV exposure, while phosphorylation of p38 already increased 30 min after OMV exposure. Phosphorylation of STAT1 was prominent after 180 min of stimulation. To investigate the involvement of TLR4 in the observed activation pattern in ECs, cells were further stimulated with *Kp*OMVs alone or in combination with PB (Fig. 4B). While *c*COMVs served as negative control. *Kp* and *c*COMVs were added to HULEC-5a cells at MOV_{1000} for 180 min with or without PB pretreatment for 1 h. Combination of *Kp*OMVs with PB blocked degradation of IRAK-1 and phosphorylation of p38. In contrast to *Kp*OMVs, *c*COMVs lacked the capacity to induce degradation of IRAK-1 along with phosphorylation of p38 (Fig. 4B).

Additionally, nuclear translocation of p65 and p38 were investigated as mean of NF-κB and p38 signaling activation and their nuclear translocation both occurred 30 min after *Kp*OMV addition (Fig. 4C). Interestingly, PB pretreatment of *Kp*OMVs reduced p65 and p38 translocation (Fig. 4D). Altogether, these results indicate that OMVs induce LPS-mediated TLR4 signaling and associated downstream activation via the MyD88/IRAK-1 axis that further results in activation of NF-κB and p38 signaling to block RNase1 in human ECs.

OMVs repress endothelial RNase1 mRNA via p38 signaling

To further identify the responsible downstream signaling pathway for OMV-mediated RNase1 repression, we performed OMV-stimulation experiments combined with signaling molecule inhibitors targeting the type I interferon- or IL-6-mediated JAK/STAT pathway (JAKi:

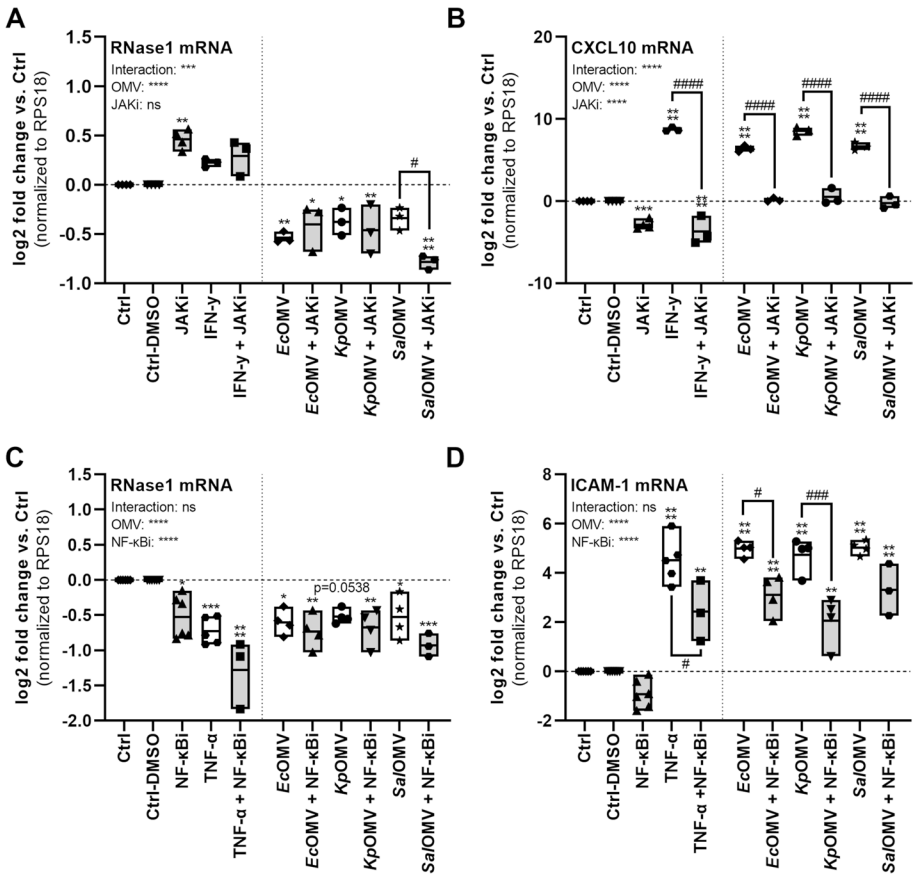

Fig. 5 OMV-mediated RNase1 mRNA repression is independent of JAK/STAT and NF-κB signaling. HULEC-5a were pretreated for 1 h with 5 μM JAKi (Ruxolitinib) or NF-κBi (BAY-11–7082) followed by 16 h stimulation with SEC-purified OMVs from *Ec*, *Kp* and *Sal* (MOV_{1000}) as well as IFN-γ (250 ng/ml) or TNF-α (10 ng/ml) as indicated, left untreated as control (Ctrl) or treated with DMSO as solvent control (Ctrl-DMSO). mRNA expression of RNase1 (**A** and **C**), **B**) CXCL10 or **D**) ICAM-1 was determined by qPCR, normalized to RPS18 and the respective Ctrl. $n = 3–6$, line at mean, Two-way ANOVA with Tukey's multiple comparison test. * compared to corresponding Ctrl, # as indicated. $^{*}p < 0.05$, $^{**}p < 0.01$, $^{***}p < 0.001$, $^{****}p < 0.0001$. $^{\#}p < 0.05$, $^{\#\#}p < 0.01$, $^{\#\#\#\#}p < 0.0001$

JAK1 inhibitor; Ruxolitinib; 5 μM), the MyD88/IRAK-1/NF-κB pathway (NF-κBi: NF-κB inhibitor; BAY11-7082; 5 μM) and the MyD88/IRAK-1/p38 pathway (p38i: p38 inhibitor; SB202190; 10 μM). Therefore, HULEC-5a were pretreated for 1 h with JAKi, NF-κBi (Fig. 5) or p38i (Fig. 6; grey bars) prior to 16 h OMV (MOV_{1000}), IFN-γ (250 ng/ml) or TNF-α (10 ng/ml) stimulation (white bars) as indicated. Untreated and DMSO treated cells served as controls (Ctrl, Ctrl-DMSO). Investigation of JAK/STAT signaling using JAKi showed a slight upregulation of RNase1 mRNA by the inhibitor itself compared to the respective controls. Additionally, IFN-γ as an initiator of JAK/STAT signaling only slightly affected RNase1 mRNA levels without reaching significance, that was not affected by JAKi treatment (Fig. 5A). In line with our previous data for STAT1 phosphorylation (Fig. 4A), RNase1 mRNA expression was repressed upon *Ec*OMV, *Kp*OMV and *Sal*OMV stimulation independent of JAKi treatment (Fig. 5A). In addition, mRNA expression of the JAK/STAT-dependent mRNA CXCL10 [49] was significantly increased upon IFN-γ and OMV treatment that was blocked to basal level by JAKi pretreatment, indicating successful pathway inhibition by the applied inhibitor (Fig. 5B). As JAK/STAT signaling seems not to be responsible for OMV-mediated RNase1 regulation, we further investigated the MyD88/IRAK-1/NF-κB pathway using NF-κBi (Fig. 5C-D). Interestingly, the inhibitor itself slightly repressed RNase1 mRNA expression and could not recover TNF-α- or OMV-mediated RNase1 repression on mRNA level. On the contrary, NF-κBi further intensified the repressive effect of TNF-α and OMVs on RNase1 expression (Fig. 5C). Functionality of the inhibitor was demonstrated by mRNA expression of NF-κB-dependent ICAM-1 [50, 51]. Here, TNF-α or OMV induced ICAM-1 mRNA expression was successfully reduced upon NF-κBi treatment compared to samples without inhibitor pretreatment (Fig. 5D).

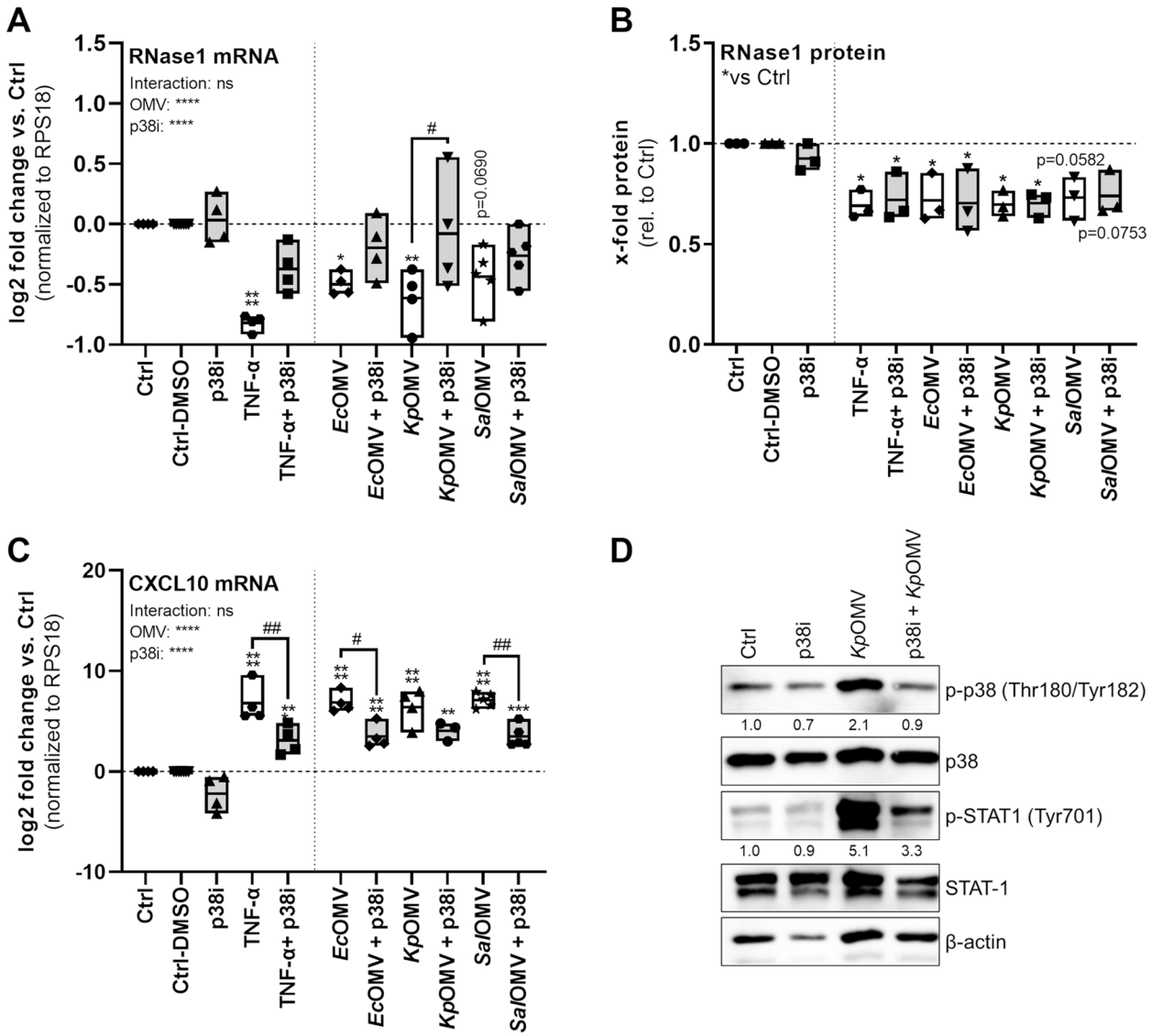

Fig. 6 OMV-mediated RNase1 mRNA repression depends on p38 signaling. HULEC-5a were pretreated for 1 h with 10 µM p38i (SB202190) followed by 16 h stimulation with SEC-purified OMVs from *Ec*, *Kp* and *Sal* (MOV_{1000}) as well as TNF-α (10 ng/ml), treated with DMSO as solvent control (Ctrl-DMSO) or left untreated as control (Ctrl). mRNA expression of **A**) RNase1 and **C**) CXCL10 was determined by qPCR, normalized to RPS18 and the respective Ctrl. $n = 3–5$, line at mean, Two-way ANOVA with Tukey's multiple comparison test. **B)** RNase1 protein release from 16 h stimulated HULEC-5a was measured by ELISA, depicted as x-fold protein relative to Ctrl. **D)** HULEC-5a were pretreated with p38i (10 µM for 1 h) followed by 180 min *Kp*OMV stimulation (MOV_{1000}). Expression and phosphorylation of p38 and STAT1 were determined by Western Blot. β-actin served as a loading control. One representative result is shown. **A, C)** $n = 4$, line at mean; Two-way ANOVA with Tukey's multiple comparison test. * compared to corresponding Ctrl, # as indicated. $^{*}p < 0.05$, $^{**}p < 0.01$, $^{***}p < 0.001$, $^{****}p < 0.0001$. $^{\#}p < 0.05$, $^{\#\#}p < 0.01$. **B)** $n = 3$, line at mean; One-way ANOVA with Tukey's multiple comparison test. $^{*}p < 0.05$

As a third potential pathway regulating OMV-mediated RNase1 repression, the MyD88/IRAK-1/p38 axis was analyzed using p38i (Fig. 6). Similar to previous data obtained with PB-pretreated OMVs, p38i preincubation (grey bars) of HULEC-5a markedly recovered RNase1 mRNA expression after treatment with TNF-α, *Ec*OMV, *Kp*OMV or *Sal*OMV (white bars) to almost basal levels compared to p38i alone or the respective controls. Furthermore, this effect even reached significance in the case of *Kp*OMVs (Fig. 6A). Interestingly, RNase1 protein secretion was significantly repressed by TNF-α and OMV exposure independent of p38i treatment, which did not rescue the protein release (Fig. 6B). In addition, TNF-α, *Ec*OMV, *Kp*OMV or *Sal*OMV induced CXCL10 mRNA expression was significantly reduced by p38i, verifying a functional

inhibition (Fig. 6C) [49, 52], which is further promoted by successful blocking of p38 phosphorylation upon *Kp*OMV treatment and reduced phosphorylation of STAT1 (Fig. 6D). Additionally, stimulation of HULEC-5a with all aforementioned stimuli and inhibitors was not cytotoxic to the cells (Fig. S3E-G).

Altogether our data provides evidence that OMV-mediated RNase1 mRNA repression is regulated via the TLR4/MyD88/IRAK-1/p38 cascade in human lung endothelial cells.

Discussion

Sepsis is a life-threatening condition caused by a deregulated immune response to infection that leads to organ dysfunction and accounts for almost 20% of all global mortalities [1, 53]. In this context, vascular dysfunction is a key feature of sepsis, which can lead to bleeding, multi-organ failure and death [8, 9, 54]. Besides the classical inflammatory mediators like cytokines or thrombotic factors, EVs were found to be key players in intercellular communication during infection [11]. Bacteria-derived EVs can be secreted into the blood stream during systemic infection, but are also able to reach the blood prior to the bacteria and disseminate further and faster [14, 55]. Moreover, they are capable of causing-sepsis like systemic inflammation [56] and are associated with complications of sepsis such as disseminated intravascular coagulation and cardiac malfunction [18, 57, 58].

To understand how bEVs influence sepsis progression and endothelial dysfunction, we investigated the impact of bEVs from the sepsis-associated pathogens *Escherichia coli*, *Klebsiella pneumoniae*, *Salmonella enterica* serovar Typhimurium and *Streptococcus pneumoniae* on RNase1, a vessel protective factor, in human lung ECs. Gram-negative OMVs from *Ec*, *Kp* and *Sal* significantly reduced RNase1 expression compared to the gram-positive MVs from *Sp*. Furthermore, we demonstrated that the OMV-mediated RNase1 repression is regulated via LPS-induced activation of the TLR4/MyD88/IRAK-1 axis, with p38 playing a crucial role in inflamed human lung ECs.

RNase1 is a vessel-protective factor that counteracts the effects of eRNA, whose downregulation is linked to various vascular pathologies, like thrombosis, myocardial infarction, atherosclerosis and stroke [30, 41]. Although insufficiently studied in bacterial infections and sepsis, RNase1 administration has been shown to block the eRNA-mediated mechanism of alveolar epithelial cell infection by *Streptococcus pneumoniae* [59]. Additionally, RNase1 levels are elevated in serum in the early disease stage of sepsis and can act as a prognostic factor for the development of multi-organ failure [43]. However, sepsis progression leads to an increase in serum levels of RNase1 antagonists, eRNA and RNase-Inhibitor, potentially repressing RNase1. Besides that, studies in mice suggest that RNase1 administration can prevent sepsis-associated tissue and organ damage [42], highlighting its potential as a therapeutic intervention. These findings, combined with the profound influence of RNase1 repression in thrombotic diseases, suggest that the RNase1-eRNA system plays a crucial role in infectious and systemic diseases like sepsis, potentially promoting disease progression and a fatal outcome.

Future investigation into RNase1 in the context of (pneumogenic) sepsis is crucial, as pneumonia is the leading cause of sepsis. To this end, we investigated the impact of bEVs from sepsis-associated pathogens on RNase1 regulation in human lung microvascular ECs (HULEC-5a) as a model system. ECs in the pulmonary microvasculature play a critical role in gas exchange [60, 61] and also act as first line of defense by initiating the immune response against invading pathogens [62].

We found that only OMVs from the gram-negative bacteria *Ec*, *Kp* and *Sal* activated the endothelium and repressed RNase1, while gram-positive MVs from *Sp* could not. The difference may be due to surface-exposed bacterial toxins, with lipoprotein being the major toxin exposed on *Sp*MVs and LPS being present on OMVs [63, 64]. Previous studies demonstrated that *Sp*MVs activated proinflammatory signaling cascades in primary human macrophages via exposed lipoprotein and TLR2 [44, 63, 65]. HULEC-5a may be insensitive to *Sp*MVs due to low TLR2 expression, whereas TLR4 is expressed and cells were more responsive to OMV-associated LPS from *Ec*, *Kp* and *Sal*. This is in line with the literature, showing low expression of TLR2 and high expression of TLR4 in dermal microvascular ECs [66].

As consequence, OMVs from *Ec*, *Kp* and *Sal* robustly activated the endothelium, that is consistent with data from macrophages [44, 67], as indicated by increased expression of the key inflammatory cytokines CXCL8 and CXCL10 and the cell adhesion molecule ICAM-1 [68, 69] and repression of RNase1 mRNA and protein. This effect might be attributed to the OMV-exposed LPS, as confirmed by treatment with Polymyxin B (PB), an LPS neutralizing peptide antibiotic [46], that could block the OMV-mediated RNase1 repression and EC activation. In comparison, OMVs from *cC* carrying a non-functional LPS did not influence RNase1 or the proinflammatory EC activation. These data are in line with literature that demonstrates a potent function of PB in blocking OMV-exposed LPS-mediated inflammation [70, 71].

The RNase1 recovering effect of PB in HULEC-5a indicated an LPS/TLR4-dependent mechanism responsible for inducing RNase1 repression. Investigation of the

underlying intracellular signaling induced by OMV stimulation of human lung ECs revealed activation of both the MyD88/IRAK-1 and TRIF axes [23–25, 68]. These findings align with literature investigating OMV-mediated signal transduction, where *Legionella pneumophila* OMVs were shown to proinflammatory activate macrophages via TLR2, IRAK-1 and NF-κB [72], while OMVs from *Porphyromonas gingivalis* mediate endothelial nitric oxide synthase suppression in human ECs via ERK1/2 and p38 signaling [73]. Interestingly, PB treatment of OMVs only blocked the activation of the MyD88/IRAK-1 axis as indicated by reduced IRAK-1 degradation, p38 phosphorylation and translocation and p65 translocation. These results point towards a MyD88/IRAK-1-dependent signaling cascade for RNase1 repression via NF-κB and p38. Similar regulations of LPS-induced TLR4 signaling and PB were obtained by Cheng et al., who demonstrated an impact of PB on LPS-induced endotoxemia in mice via the TLR4/MyD88 axis [74]. Signaling pathway inhibitors targeting specific downstream molecules of TLR4 were used for verification. The JAK1 inhibitor Ruxolitinib was used to investigate the TLR4/IRF axis that provokes activation of IFN signaling via JAK1/STAT1 [23–25]. However, Ruxolitinib treatment of HULEC-5a prior to OMV stimulation did not prevent RNase1 repression and Ruxolitinib treatment alone increased RNase1 expression. Little is known about the underlying molecular pathways of RNase1 regulation in ECs, but referred data primarily focused on p38 and histone deacetylase 2 (HDAC2)-mediated mechanisms [35, 36]. Besides the possibility of off-target effects of Ruxolitinib, JAK1 can also be associated to IL-6 signaling [75]. Unpublished data by our group suggest that HULEC-5a produce IL-6 in response to OMV stimulation, and IL-6/IL-6R treatment represses RNase1. Thus, it might be possible that JAK1 can be associated to RNase1 signaling via an autocrine feedback loop in which OMVs trigger the release of IL-6 via TLR4/NF-κB/p38 signaling [68, 76, 77]. This in turn can reduce RNase1 expression via JAK1 as well as self-perpetuates IL-6 to promote persistent inflammation. As IL-6 is also known as a key inflammatory mediator during cytokine storm in sepsis [2], further investigation of a possible impact of Ruxolitinib, JAK1 and IL-6 in RNase1-associated EC dysfunction might be of future interest. Thereby, Ruxolitinib could be suitable to prevent sepsis-associated IL-6 release to impede EC dysfunction via promoting RNase1 expression.

As the downstream signaling of TLR4/MyD88/IRAK-1 can either be mediated via NF-κB or p38, we further investigated the impact of these on OMV-mediated RNase1 repression using BAY11-7082 as NF-κB inhibitor and SB202190 as p38 inhibitor. BAY11-7082 itself slightly downregulated RNase1 and elevated the repressive effect of TNF-α and OMVs. However, previous studies by Gansler et al. and our group did not observe any impact of NF-κB inhibition on RNase1 mRNA expression in primary human umbilical vein ECs [34, 35]. Furthermore, JNK signaling was found to be important for physiological RNase1 expression, as JNK inhibition repressed RNase1 [35]. These findings suggest that RNase1 regulation in ECs may be organ-specific and vary depending on the physiological demands of the vascular bed [78–81]. ECs from different organs can activate organ-specific pathways and express organ-specific transporters and surface markers [60], and even within a specific vascular bed, there can be differences in EC function [82]. This heterogeneity may explain differences in reactivity of the microvascular lung endothelium used in this study compared to ECs from the large umbilical vein used in previous studies addressing RNase1 regulations.

Compared to these findings, blocking the p38 signaling cascade with SB202190 recovered RNase1 mRNA, indicating that OMV-mediated TLR4 activation signals via MAPK p38 to repress RNase1 expression which is in line with previous studies on TNF-α-mediated RNase1 mRNA repression [35]. TNF-α is a major regulator of RNase1 [39, 41, 83, 84] and can repress it through activation of an HDAC2-containing NuRD repressor complex, which deacetylates the *RNASE1* promoter region and prevents RNase1 transcription [36]. This pathway is mediated via p38 signaling as its inhibition impedes repressor complex recruitment and *RNASE1* chromatin modulation upon TNF-α stimulation [35, 36]. Therefore, p38 MAPK negatively regulates gene expression and is associated with known RNase1 repressive stimuli like TNF-α or IL-1β as well as LPS [35, 85–87]. Although RNase1 mRNA expression was recovered by p38 inhibition, its protein release was still affected by OMVs as well as TNF-α treatment. As p38 is known as a major regulator of intracellular signaling, inhibition of this pathway can also influence a variety of cellular factors that might trigger RNase1 repression [85, 86, 88, 89]. Based on our data we conclude that an unknown factor that acts downstream of TLR4 affects RNase1 protein release, as PB treatment efficiently recovered RNase1 protein upon OMV stimulation. However, further investigation needs to be done to maintain RNase1 integrity in the inflamed endothelium. The presented results provide strong evidence for a p38-mediated RNase1 mRNA regulation upon OMV treatment and identify p38 as a key repressor of RNase1, consistent with our previously published data on TNF-α mediated RNase1 regulation [35, 36].

Furthermore, our study suggests potential therapeutic strategies for sepsis-associated vascular dysfunction by restoring RNase1 function and vascular homeostasis. While p38 inhibitors have shown promise in clinical

trials [90–93] by decreasing serum levels of proinflammatory cytokines [94], our data indicates that p38 inhibition alone might not be sufficient to restore RNase1 function and vascular integrity. Thus, a combination of p38 inhibitors with other complementary therapeutic options should be considered. One particularly interesting option is PB treatment, as it represents an approved drug and has already been investigated in several clinical trials for sepsis intervention, where it improved various clinical outcomes, such as mean arterial pressure, ventilator-free days, and mortality [95–99]. PB treatment fully recovered RNase1 mRNA and protein and has been shown to reduce the proapoptotic function of plasma of septic patients in sepsis-induced acute renal failure [100]. Additionally, new innovations such as PB-releasing nanoparticles have been developed to target bacterial accumulation and vascular inflammation [101] and thereby could be a valuable tool for sepsis intervention through RNase1 recovery in human ECs.

Conclusions

In summary, we observed that EVs released by different gram-negative, (pneumogenic) sepsis-associated bacteria repress RNase1, a key modulator of vascular integrity, in human lung microvascular ECs. This effect is mediated via signaling through TLR4/MyD88/IRAK-1 and p38 and can be prevented by LPS neutralization via PB and in part p38 inhibition. Thereby, our data provides new insights in the regulation of sepsis-induced vascular dysfunction and offers novel treatment options to prevent sepsis-associated RNase1 repression and consecutive vascular breakdown.

Abbreviations

bEVs	Bacterial extracellular vesicles
cC	*Clear Coli*
CXCL8	C-X-C motif chemokine ligand 8
CXCL10	C-X-C motif chemokine ligand 10
DMSO	Dimethyl sulfoxide
Ec	*Escherichia coli*
eRNA	Extracellular RNA
EVs	Extracellular vesicles
HDAC2	Histone deacetylase 2
ICAM-1	Intercellular adhesion molecule 1
IFN	Interferon
IFNAR	Interferon alpha/beta receptor
JAKi	Janus activated kinase inhibitor (Ruxolitinib)
Kp	*Klebsiella pneumoniae*
LDH	Lactate dehydrogenase
LPS	Lipopolysaccharide
MAPK	Mitogen activated protein kinase
MVs	Membrane vesicles
NF-κBi	Nuclear factor kappa B inhibitor (BAY11-7081)
OMVs	Outer membrane vesicles
p38i	P38 inhibitor (SB202190)
PB	Polymyxin B
qPCR	Quantitative reverse transcription PCR
RNase1	Ribonuclease 1
Sal	*Salmonella enterica* serovar Typhimurium
Sp	*Streptococcus pneumoniae*
TLR	Toll-like receptor
TNF-α	Tumor necrosis factor alpha
UF-SEC	Ultrafiltration and size exclusion chromatography

Supplementary Information

The online version contains supplementary material available at https://doi.org/10.1186/s12964-023-01131-2.

Additional file 1: Figure S1. OMV-mediated intracellular signaling cascades. **Figure S2.** Isolation procedure and characterization of bEVs. **Figure S3.** Impact of OMVs and inhibitor treatments on HULEC-5a. **Figure S4.** SpMVs do not activate human lung ECs. **Figure S5.** Basal TLR2 and TLR4 mRNA expression in human lung ECs.

Acknowledgements

We thank Sabrina von Einem for her help in editing and proof reading the manuscript and all other lab members for support and discussion. All graphical illustrations were created with BioRender.com.

Authors' contributions

KL, BS, ALJ contributed to conception and design of the study; KL, JME, MH, MW, JB, IB, performed experiments; CP performed vesicle quantification; TH performed TEM; KL, JME, MH, IB, ALJ analyzed the data; KL, ALJ created the figures; KL, ALJ wrote the manuscript; all authors contributed to manuscript revision, read and approved the submitted version.

Funding

Open Access funding enabled and organized by Projekt DEAL. Parts of this work were funded by the Von-Behring Röntgen-Stiftung (69–0012) to KL, the Hessisches Ministerium für Wissenschaft und Kunst (LOEWE Diffusible Signals) to BS and ALJ, the German Ministry for Education and Research (BMBF) (ERACo-SysMed2 SysMed-COPD-FKZ 031L0140, PerMedCOPD-FKZ 01EK2203A) to BS, the Von-Behring Röntgen-Stiftung (66-LV07) to BS and the Deutsche Forschungsgemeinschaft (SFB/TR-84 TP C01) to BS.

Declarations

Competing interests

All authors declare that they have no known competing financial interests or personal relationships that could have appeared to influence the work reported in this paper.

Author details

[1]Institute for Lung Research, Universities of Giessen and Marburg Lung Center, Philipps-University Marburg, German Center for Lung Research (DZL), Marburg, Germany. [2]Institute for Tumor Immunology and Core Facility – Extracellular Vesicles, Philipps-University Marburg, Marburg, Germany. [3]Center for Synthetic Microbiology (SYNMIKRO), Philipps-University Marburg, Marburg, Germany. [4]Core Facility Flow Cytometry – Bacterial Vesicles, Philipps-University Marburg, Marburg, Germany. [5]Department of Pulmonary and Critical Care Medicine, Philipps-University Marburg, Marburg, Germany. [6]Member of the German Center for Infectious Disease Research (DZIF), Marburg, Germany.

Received: 8 March 2023 Accepted: 17 April 2023
Published online: 15 May 2023

References

1. Rudd KE, Johnson SC, Agesa KM, Shackelford KA, Tsoi D, Kievlan DR, et al. Global, regional, and national sepsis incidence and mortality, 1990–2017: analysis for the Global Burden of Disease Study. Lancet. 2020;395:200–11. https://doi.org/10.1016/S0140-6736(19)32989-7.

2. Chousterman BG, Swirski FK, Weber GF. Cytokine storm and sepsis disease pathogenesis. Semin Immunopathol. 2017;39:517–28. https://doi.org/10.1007/s00281-017-0639-8.
3. Feldman C, Anderson R. Pneumonia as a systemic illness. Curr Opin Pulm Med. 2018;24:237–43. https://doi.org/10.1097/MCP.0000000000000466.
4. Minasyan H. Sepsis: mechanisms of bacterial injury to the patient. Scand J Trauma Resusc Emerg Med. 2019;27:19. https://doi.org/10.1186/s13049-019-0596-4.
5. Iba T, Levi M, Levy JH. Sepsis-induced coagulopathy and disseminated intravascular coagulation. Semin Thromb Hemost. 2020;46:89–95. https://doi.org/10.1055/s-0039-1694995.
6. Luyt CE, Hekimian G, Koulenti D, Chastre J. Microbial cause of ICU-acquired pneumonia: hospital-acquired pneumonia versus ventilator-associated pneumonia. Curr Opin Crit Care. 2018;24:332–8. https://doi.org/10.1097/MCC.0000000000000526.
7. Prina E, Ranzani OT, Torres A. Community-acquired pneumonia. Lancet. 2015;386:1097–108. https://doi.org/10.1016/S0140-6736(15)60733-4.
8. Cecconi M, Evans L, Levy M, Rhodes A. Sepsis and septic shock. Lancet. 2018;392:75–87. https://doi.org/10.1016/S0140-6736(18)30696-2.
9. Hotchkiss RS, Karl IE. The pathophysiology and treatment of sepsis. N Engl J Med. 2003;348:138–50. https://doi.org/10.1056/NEJMra021333.
10. Terrasini N, Lionetti V. Exosomes in critical illness. Crit Care Med. 2017;45:1054–60. https://doi.org/10.1097/CCM.0000000000002328.
11. Jung AL, Schmeck B, Wiegand M, Bedenbender K, Benedikter BJ. The clinical role of host and bacterial-derived extracellular vesicles in pneumonia. Adv Drug Deliv Rev. 2021. https://doi.org/10.1016/j.addr.2021.05.021.
12. Doyle LM, Wang MZ. Overview of extracellular vesicles, their origin, composition, purpose, and methods for exosome isolation and analysis. Cells. 2019. https://doi.org/10.3390/cells8070727.
13. Maas SLN, Breakefield XO, Weaver AM. Extracellular vesicles: unique intercellular delivery vehicles. Trends Cell Biol. 2017;27:172–88. https://doi.org/10.1016/j.tcb.2016.11.003.
14. Bittel M, Reichert P, Sarfati I, Dressel A, Leikam S, Uderhardt S, et al. Visualizing transfer of microbial biomolecules by outer membrane vesicles in microbe-host-communication in vivo. J Extracell Vesicles. 2021;10:e12159. https://doi.org/10.1002/jev2.12159.
15. Joffre J, Hellman J, Ince C, Ait-Oufella H. Endothelial responses in sepsis. Am J Respir Crit Care Med. 2020;202:361–70. https://doi.org/10.1164/rccm.201910-1911TR.
16. Lubkin A, Torres VJ. Bacteria and endothelial cells: a toxic relationship. Curr Opin Microbiol. 2017;35:58–63. https://doi.org/10.1016/j.mib.2016.11.008.
17. Shah B, Sullivan CJ, Lonergan NE, Stanley S, Soult MC, Britt LD. Circulating bacterial membrane vesicles cause sepsis in rats. Shock. 2012;37:621–8. https://doi.org/10.1097/SHK.0b013e318250de5d.
18. Svennerholm K, Park K-S, Wikström J, Lässer C, Crescitelli R, Shelke GV, et al. Escherichia coli outer membrane vesicles can contribute to sepsis induced cardiac dysfunction. Sci Rep-Uk. 2017;7:17434. https://doi.org/10.1038/s41598-017-16363-9.
19. Yu YJ, Wang XH, Fan GC. Versatile effects of bacterium-released membrane vesicles on mammalian cells and infectious/inflammatory diseases. Acta Pharmacol Sin. 2018;39:514–33. https://doi.org/10.1038/aps.2017.82.
20. Zhang Y, Meng H, Ma RS, He ZX, Wu XM, Cao MH, et al. Circulating microparticles, blood cells, and endothelium induce procoagulant activity in sepsis through phosphatidylserine exposure. Shock. 2016;45:299–307. https://doi.org/10.1097/Shk.0000000000000509.
21. Toyofuku M, Nomura N, Eberl L. Types and origins of bacterial membrane vesicles. Nat Rev Microbiol. 2019;17:13–24. https://doi.org/10.1038/s41579-018-0112-2.
22. Soult MC, Lonergan NE, Shah B, Kim WK, Britt LD, Sullivan CJ. Outer membrane vesicles from pathogenic bacteria initiate an inflammatory response in human endothelial cells. J Surg Res. 2013;184:458–66. https://doi.org/10.1016/j.jss.2013.05.035.
23. Gay NJ, Symmons MF, Gangloff M, Bryant CE. Assembly and localization of Toll-like receptor signalling complexes. Nat Rev Immunol. 2014;14:546–58. https://doi.org/10.1038/nri3713.
24. Majoros A, Platanitis E, Kernbauer-Hölzl E, Rosebrock F, Müller M, Decker T. Canonical and non-canonical aspects of JAK-STAT signaling: lessons from interferons for cytokine responses. Front Immunol. 2017;8:29. https://doi.org/10.3389/fimmu.2017.00029.
25. Rathinam VAK, Zhao Y, Shao F. Innate immunity to intracellular LPS. Nat Immunol. 2019;20:527–33. https://doi.org/10.1038/s41590-019-0368-3.
26. Bochenek ML, Schafer K. Role of endothelial cells in acute and chronic thrombosis. Hamostaseologie. 2019;39:128–39. https://doi.org/10.1055/s-0038-1675614.
27. Rajendran P, Rengarajan T, Thangavel J, Nishigaki Y, Sakthisekaran D, Sethi G, Nishigaki I. The vascular endothelium and human diseases. Int J Biol Sci. 2013;9:1057–69. https://doi.org/10.7150/ijbs.7502.
28. Pober JS, Sessa WC. Evolving functions of endothelial cells in inflammation. Nat Rev Immunol. 2007;7:803–15. https://doi.org/10.1038/nri2171.
29. Wang M, Hao HF, Leeper NJ, Zhu LY, Comm EC. Thrombotic regulation from the endothelial cell perspectives. Arterioscl Throm Vas. 2018;38:E90–5. https://doi.org/10.1161/Atvbaha.118.310367.
30. Bedenbender K, Schmeck BT. Endothelial ribonuclease 1 in cardiovascular and systemic inflammation. Front Cell Dev Biol. 2020;8:576491. https://doi.org/10.3389/fcell.2020.576491.
31. Fischer S, Nishio M, Dadkhahi S, Gansler J, Saffarzadeh M, Shibamiyama A, et al. Expression and localisation of vascular ribonucleases in endothelial cells. Thromb Haemost. 2011;105:345–55. https://doi.org/10.1160/TH10-06-0345.
32. Futami J, Tsushima Y, Murato Y, Tada H, Sasaki J, Seno M, Yamada H. Tissue-specific expression of pancreatic-type RNases and RNase inhibitor in humans. DNA Cell Biol. 1997;16:413–9. https://doi.org/10.1089/dna.1997.16.413.
33. Landre JB, Hewett PW, Olivot JM, Friedl P, Ko Y, Sachinidis A, Moenner M. Human endothelial cells selectively express large amounts of pancreatic-type ribonuclease (RNase 1). J Cell Biochem. 2002;86:540–52. https://doi.org/10.1002/jcb.10234.
34. Gansler J, Preissner KT, Fischer S. Influence of proinflammatory stimuli on the expression of vascular ribonuclease 1 in endothelial cells. FASEB J. 2014;28:752–60. https://doi.org/10.1096/fj.13-238600.
35. Bedenbender K, Beinborn I, Vollmeister E, Schmeck B. p38 and Casein Kinase 2 Mediate Ribonuclease 1 Repression in Inflamed Human Endothelial Cells via Promoter Remodeling Through Nucleosome Remodeling and Deacetylase Complex. Front Cell Dev Biol. 2020;8:604. https://doi.org/10.3389/fcell.2020.563604.
36. Bedenbender K, Scheller N, Fischer S, Leiting S, Preissner KT, Schmeck BT, Vollmeister E. Inflammation-mediated deacetylation of the ribonuclease 1 promoter via histone deacetylase 2 in endothelial cells. FASEB J. 2019;33:9017–29. https://doi.org/10.1096/fj.201900451R.
37. Fischer S, Preissner KT. Extracellular nucleic acids as novel alarm signals in the vascular system Mediators of defence and disease. Hamostaseologie. 2013;33:37–42. https://doi.org/10.5482/Hamo-13-01-0001.
38. Garnett ER, Lomax JE, Mohammed BM, Gailani D, Sheehan JP, Raines RT. Phenotype of ribonuclease 1 deficiency in mice. RNA. 2019;25:921–34. https://doi.org/10.1261/rna.070433.119.
39. Kannemeier C, Shibamiya A, Nakazawa F, Trusheim H, Ruppert C, Markart P, et al. Extracellular RNA constitutes a natural procoagulant cofactor in blood coagulation. Proc Natl Acad Sci U S A. 2007;104:6388–93. https://doi.org/10.1073/pnas.0608647104.
40. Simsekyilmaz S, Cabrera-Fuentes HA, Meiler S, Kostin S, Baumer Y, Liehn EA, et al. Role of extracellular RNA in atherosclerotic plaque formation in mice. Circulation. 2014;129:598–606. https://doi.org/10.1161/CIRCULATIONAHA.113.002562.
41. Zernecke A, Preissner KT. Extracellular Ribonucleic Acids (RNA) Enter the Stage in Cardiovascular Disease. Circ Res. 2016;118:469–79. https://doi.org/10.1161/CIRCRESAHA.115.307961.
42. Zechendorf E, O'Riordan CE, Stiehler L, Wischmeyer N, Chiazza F, Collotta D, et al. Ribonuclease 1 attenuates septic cardiomyopathy and cardiac apoptosis in a murine model of polymicrobial sepsis. JCI Insight. 2020. https://doi.org/10.1172/jci.insight.131571.
43. Martin L, Koczera P, Simons N, Zechendorf E, Hoeger J, Marx G, Schuerholz T. The Human Host Defense Ribonucleases 1, 3 and 7 Are Elevated in Patients with Sepsis after Major Surgery–A Pilot Study. Int J Mol Sci. 2016;17:294. https://doi.org/10.3390/ijms17030294.
44. Bierwagen J, Wiegand M, Laakmann K, Danov O, Limburg H, Herbel SM, Heimerl T, Dorna J, Jonigk D, Preußer C, Bertrams W, Braun A, Sewald K, Schulte LN, Bauer S, Pogge von Strandmann E, Böttcher-Friebertshäuser E, Schmeck B, Jung AL. Bacterial vesicles block viral replication in

macrophages via TLR4-TRIF-axis. Cell Commun Signal. 2023;21(1):65. https://doi.org/10.1186/s12964-023-01086-4.
45. Livak KJ, Schmittgen TD. Analysis of relative gene expression data using real-time quantitative PCR and the 2(T)(-Delta Delta C) method. Methods. 2001;25:402–8. https://doi.org/10.1006/meth.2001.1262.
46. Goode A, Yeh V, Bonev BB. Interactions of polymyxin B with lipopolysaccharide-containing membranes. Faraday Discuss. 2021;232:317–29. https://doi.org/10.1039/d1fd00036e.
47. Cardoso LS, Araujo MI, Góes AM, Pacífico LG, Oliveira RR, Oliveira SC. Polymyxin B as inhibitor of LPS contamination of Schistosoma mansoni recombinant proteins in human cytokine analysis. Microb Cell Fact. 2007;6:1. https://doi.org/10.1186/1475-2859-6-1.
48. Mamat U, Woodard RW, Wilke K, Souvignier C, Mead D, Steinmetz E, et al. Endotoxin-free protein production—ClearColi™ technology. Nat Methods. 2013;10:916. https://doi.org/10.1038/nmeth.f.367.
49. Liu M, Guo S, Hibbert JM, Jain V, Singh N, Wilson NO, Stiles JK. CXCL10/IP-10 in infectious diseases pathogenesis and potential therapeutic implications. Cytokine Growth Factor Rev. 2011;22:121–30. https://doi.org/10.1016/j.cytogfr.2011.06.001.
50. Xue J, Thippegowda PB, Hu G, Bachmaier K, Christman JW, Malik AB, Tiruppathi C. NF-kappaB regulates thrombin-induced ICAM-1 gene expression in cooperation with NFAT by binding to the intronic NF-kappaB site in the ICAM-1 gene. Physiol Genomics. 2009;38:42–53. https://doi.org/10.1152/physiolgenomics.00012.2009.
51 Holden NS, Catley MC, Cambridge LM, Barnes PJ, Newton R. ICAM-1 expression is highly NF-kappaB-dependent in A549 cells. No role for ERK and p38 MAPK. Eur J Biochem. 2004;271:785–91. https://doi.org/10.1111/j.1432-1033.2004.03982.x.
52. Xia J-B, Mao C-Z, Chen Z-Y, Liu G-H, Wu H-Y, Zhou D-C, et al. The CXCL10/CXCR3 axis promotes cardiac microvascular endothelial cell migration via the p38/FAK pathway in a proliferation-independent manner. Exp Mol Pathol. 2016;100:257–65. https://doi.org/10.1016/j.yexmp.2016.01.010.
53. Singer M, Deutschman CS, Seymour CW, Shankar-Hari M, Annane D, Bauer M, et al. The Third International Consensus Definitions for Sepsis and Septic Shock (Sepsis-3). JAMA. 2016;315:801–10. https://doi.org/10.1001/jama.2016.0287.
54. Greco E, Lupia E, Bosco O, Vizio B, Montrucchio G. Platelets and Multi-Organ Failure in Sepsis. Int J Mol Sci. 2017. https://doi.org/10.3390/ijms18102200.
55. Michel LV, Gaborski T. Outer membrane vesicles as molecular biomarkers for Gram-negative sepsis: taking advantage of nature's perfect packages. J Biol Chem. 2022;298:102483. https://doi.org/10.1016/j.jbc.2022.102483.
56. Park K-S, Lee J, Lee C, Park HT, Kim J-W, Kim OY, et al. Sepsis-like systemic inflammation induced by nano-sized extracellular vesicles from feces. Front Microbiol. 2018;9:1735. https://doi.org/10.3389/fmicb.2018.01735.
57. Wang E, Liu Y, Qiu X, Tang Y, Wang H, Xiao X, et al. Bacteria-released outer membrane vesicles promote disseminated intravascular coagulation. Thromb Res. 2019;178:26–33. https://doi.org/10.1016/j.thromres.2019.03.019.
58. Peng Y, Gao M, Liu Y, Qiu X, Cheng X, Yang X, et al. Bacterial outer membrane vesicles induce disseminated intravascular coagulation through the caspase-11-gasdermin D pathway. Thromb Res. 2020;196:159–66. https://doi.org/10.1016/j.thromres.2020.08.013.
59. Zakrzewicz D, Bergmann S, Didiasova M, Giaimo BD, Borggrefe T, Mieth M, et al. Host-derived extracellular RNA promotes adhesion of Streptococcus pneumoniae to endothelial and epithelial cells. Sci Rep. 2016;6:37758. https://doi.org/10.1038/srep37758.
60. Jambusaria A, Hong Z, Zhang L, Srivastava S, Jana A, Toth PT, et al. Endothelial heterogeneity across distinct vascular beds during homeostasis and inflammation. Elife. 2020. https://doi.org/10.7554/eLife.51413.
61. Tsuchiya T, Doi R, Obata T, Hatachi G, Nagayasu T. Lung Microvascular Niche, Repair, and Engineering. Front Bioeng Biotechnol. 2020;8:105. https://doi.org/10.3389/fbioe.2020.00105.
62. Amersfoort J, Eelen G, Carmeliet P. Immunomodulation by endothelial cells - partnering up with the immune system? Nat Rev Immunol. 2022;22:576–88. https://doi.org/10.1038/s41577-022-00694-4.
63. Briaud P, Carroll RK. Extracellular vesicle biogenesis and functions in gram-positive bacteria. Infect Immun. 2020. https://doi.org/10.1128/IAI.00433-20.
64. Ellis TN, Kuehn MJ. Virulence and immunomodulatory roles of bacterial outer membrane vesicles. Microbiol Mol Biol Rev. 2010;74:81–94. https://doi.org/10.1128/MMBR.00031-09.
65. Volgers C, Benedikter BJ, Grauls GE, Savelkoul PHM, Stassen FRM. Immunomodulatory role for membrane vesicles released by THP-1 macrophages and respiratory pathogens during macrophage infection. BMC Microbiol. 2017;17:216. https://doi.org/10.1186/s12866-017-1122-3.
66. Faure E, Equils O, Sieling PA, Thomas L, Zhang FX, Kirschning CJ, et al. Bacterial lipopolysaccharide activates NF-kappaB through toll-like receptor 4 (TLR-4) in cultured human dermal endothelial cells. Differential expression of TLR-4 and TLR-2 in endothelial cells. J Biol Chem. 2000;275:11058–63. https://doi.org/10.1074/jbc.275.15.11058.
67. Watanabe S, Kumazawa Y, Inoue J. Liposomal lipopolysaccharide initiates TRIF-dependent signaling pathway independent of CD14. PLoS ONE. 2013;8:e60078. https://doi.org/10.1371/journal.pone.0060078.
68. Ciesielska A, Matyjek M, Kwiatkowska K. TLR4 and CD14 trafficking and its influence on LPS-induced pro-inflammatory signaling. Cell Mol Life Sci. 2021;78:1233–61. https://doi.org/10.1007/s00018-020-03656-y.
69. Dauphinee SM, Karsan A. Lipopolysaccharide signaling in endothelial cells. Lab Invest. 2006;86:9–22. https://doi.org/10.1038/labinvest.3700366.
70. Pfalzgraff A, Correa W, Heinbockel L, Schromm AB, Lübow C, Gisch N, et al. LPS-neutralizing peptides reduce outer membrane vesicle-induced inflammatory responses. Biochim Biophys Acta Mol Cell Biol Lipids. 2019;1864:1503–13. https://doi.org/10.1016/j.bbalip.2019.05.018.
71. Kim Y-S, Choi E-J, Lee W-H, Choi S-J, Roh T-Y, Park J, et al. Extracellular vesicles, especially derived from Gram-negative bacteria, in indoor dust induce neutrophilic pulmonary inflammation associated with both Th1 and Th17 cell responses. Clin Exp Allergy. 2013;43:443–54. https://doi.org/10.1111/cea.12085.
72. Herkt CE, Caffrey BE, Surmann K, Blankenburg S, Gesell Salazar M, Jung AL, et al. A MicroRNA Network Controls Legionella pneumophila Replication in Human Macrophages via LGALS8 and MX1. MBio. 2020;11:e03155-e3219. https://doi.org/10.1128/mBio.03155-19.
73. Jia Y, Guo B, Yang W, Zhao Q, Jia W, Wu Y. Rho kinase mediates Porphyromonas gingivalis outer membrane vesicle-induced suppression of endothelial nitric oxide synthase through ERK1/2 and p38 MAPK. Arch Oral Biol. 2015;60:488–95. https://doi.org/10.1016/j.archoralbio.2014.12.009.
74. Cheng Y, Du J, Han J, Sun W, Gao F, Zhang P, et al. Polymyxin B Attenuates LPS-Induced Death but Aggravates Radiation-Induced Death via TLR4-Myd88-IL-6 Pathway. Cell Physiol Biochem. 2017;42:1120–6. https://doi.org/10.1159/000478767.
75. Huarte E, Peel MT, Verbist K, Fay BL, Bassett R, Albeituni S, et al. Ruxolitinib, a JAK1/2 Inhibitor, Ameliorates Cytokine Storm in Experimental Models of Hyperinflammation Syndrome. Front Pharmacol. 2021;12:650295. https://doi.org/10.3389/fphar.2021.650295.
76. Kawai T, Akira S. Toll-like receptors and their crosstalk with other innate receptors in infection and immunity. Immunity. 2011;34:637–50. https://doi.org/10.1016/j.immuni.2011.05.006.
77. Medzhitov R, Horng T. Transcriptional control of the inflammatory response. Nat Rev Immunol. 2009;9:692–703. https://doi.org/10.1038/nri2634.
78. Hennigs JK, Matuszcak C, Trepel M, Körbelin J. Vascular endothelial cells: heterogeneity and targeting approaches. Cells. 2021. https://doi.org/10.3390/cells10102712.
79. Kvietys PR, Granger DN. Endothelial cell monolayers as a tool for studying microvascular pathophysiology. Am J Physiol. 1997;273:G1189–99. https://doi.org/10.1152/ajpgi.1997.273.6.G1189.
80. Marziano C, Genet G, Hirschi KK. Vascular endothelial cell specification in health and disease. Angiogenesis. 2021;24:213–36. https://doi.org/10.1007/s10456-021-09785-7.
81. Trimm E, Red-Horse K. Vascular endothelial cell development and diversity. Nat Rev Cardiol. 2023;20:197–210. https://doi.org/10.1038/s41569-022-00770-1.
82. Gillich A, Zhang F, Farmer CG, Travaglini KJ, Tan SY, Gu M, et al. Capillary cell-type specialization in the alveolus. Nature. 2020;586:785–9. https://doi.org/10.1038/s41586-020-2822-7.
83. Cabrera-Fuentes HA, Ruiz-Meana M, Simsekyilmaz S, Kostin S, Inserte J, Saffarzadeh M, et al. RNase1 prevents the damaging interplay between

extracellular RNA and tumour necrosis factor-alpha in cardiac ischaemia/reperfusion injury. Thromb Haemost. 2014;112:1110–9. https://doi.org/10.1160/TH14-08-0703.
84. Cabrera-Fuentes HA, Niemann B, Grieshaber P, Wollbrueck M, Gehron J, Preissner KT, Boning A. RNase1 as a potential mediator of remote ischaemic preconditioning for cardioprotectiondagger. Eur J Cardiothorac Surg. 2015;48:732–7. https://doi.org/10.1093/ejcts/ezu519.
85. Ashwell JD. The many paths to p38 mitogen-activated protein kinase activation in the immune system. Nat Rev Immunol. 2006;6:532–40. https://doi.org/10.1038/nri1865.
86. Ono K, Han J. The p38 signal transduction pathway: activation and function. Cell Signal. 2000;12:1–13. https://doi.org/10.1016/S0898-6568(99)00071-6.
87. Raingeaud J, Gupta S, Rogers JS, Dickens M, Han J, Ulevitch RJ, Davis RJ. Pro-inflammatory cytokines and environmental stress cause p38 mitogen-activated protein kinase activation by dual phosphorylation on tyrosine and threonine. J Biol Chem. 1995;270:7420–6. https://doi.org/10.1074/jbc.270.13.7420.
88. Miyazawa K, Mori A, Miyata H, Akahane M, Ajisawa Y, Okudaira H. Regulation of interleukin-1beta-induced interleukin-6 gene expression in human fibroblast-like synoviocytes by p38 mitogen-activated protein kinase. J Biol Chem. 1998;273:24832–8. https://doi.org/10.1074/jbc.273.38.24832.
89. Marie C, Roman-Roman S, Rawadi G. Involvement of mitogen-activated protein kinase pathways in interleukin-8 production by human monocytes and polymorphonuclear cells stimulated with lipopolysaccharide or Mycoplasma fermentans membrane lipoproteins. Infect Immun. 1999;67:688–93. https://doi.org/10.1128/IAI.67.2.688-693.1999.
90. Christie JD, Vaslef S, Chang PK, May AK, Gunn SR, Yang S, et al. A Randomized dose-escalation study of the safety and anti-inflammatory activity of the p38 mitogen-activated protein kinase inhibitor dilmapimod in severe trauma subjects at risk for acute respiratory distress syndrome. Crit Care Med. 2015;43:1859–69. https://doi.org/10.1097/CCM.0000000000001132.
91. Kumar S, Boehm J, Lee JC. p38 map kinases: Key signalling molecules as therapeutic targets for inflammatory diseases. Nat Rev Drug Discov. 2003;2:717–26. https://doi.org/10.1038/nrd1177.
92. Patnaik A, Haluska P, Tolcher AW, Erlichman C, Papadopoulos KP, Lensing JL, et al. A First-in-Human Phase I Study of the Oral p38 MAPK Inhibitor, Ralimetinib (LY2228820 Dimesylate), in Patients with Advanced Cancer. Clin Cancer Res. 2016;22:1095–102. https://doi.org/10.1158/1078-0432.CCR-15-1718.
93. Cheriyan J, Webb AJ, Sarov-Blat L, Elkhawad M, Wallace SML, Mäki-Petäjä KM, et al. Inhibition of p38 mitogen-activated protein kinase improves nitric oxide-mediated vasodilatation and reduces inflammation in hypercholesterolemia. Circulation. 2011;123:515–23. https://doi.org/10.1161/CIRCULATIONAHA.110.971986.
94. Fijen JW, Zijlstra JG, de Boer P, Spanjersberg R, Tervaert JW, van der Werf TS, et al. Suppression of the clinical and cytokine response to endotoxin by RWJ-67657, a p38 mitogen-activated protein-kinase inhibitor, in healthy human volunteers. Clin Exp Immunol. 2001;124:16–20. https://doi.org/10.1046/j.1365-2249.2001.01485.x.
95. Srisawat N, Tungsanga S, Lumlertgul N, Komaenthammasophon C, Peerapornratana S, Thamrongsat N, et al. The effect of polymyxin B hemoperfusion on modulation of human leukocyte antigen DR in severe sepsis patients. Crit Care. 2018;22:279. https://doi.org/10.1186/s13054-018-2077-y.
96. Yaroustovsky M, Abramyan M, Komardina E, Nazarova H, Popov D, Plyushch M, et al. Selective LPS Adsorption Using Polymyxin B-Immobilized Fiber Cartridges in Sepsis Patients Following Cardiac Surgery. Shock. 2018;49:658–66. https://doi.org/10.1097/SHK.0000000000001016.
97. Klein DJ, Foster D, Schorr CA, Kazempour K, Walker PM, Dellinger RP. The EUPHRATES trial (Evaluating the Use of Polymyxin B Hemoperfusion in a Randomized controlled trial of Adults Treated for Endotoxemia and Septic shock): study protocol for a randomized controlled trial. Trials. 2014;15:218. https://doi.org/10.1186/1745-6215-15-218.
98. Dellinger RP, Bagshaw SM, Antonelli M, Foster DM, Klein DJ, Marshall JC, et al. Effect of Targeted Polymyxin B Hemoperfusion on 28-Day Mortality in Patients With Septic Shock and Elevated Endotoxin Level: The EUPHRATES Randomized Clinical Trial. JAMA. 2018;320:1455–63. https://doi.org/10.1001/jama.2018.14618.
99. Klein DJ, Foster D, Walker PM, Bagshaw SM, Mekonnen H, Antonelli M. Polymyxin B hemoperfusion in endotoxemic septic shock patients without extreme endotoxemia: a post hoc analysis of the EUPHRATES trial. Intensive Care Med. 2018;44:2205–12. https://doi.org/10.1007/s00134-018-5463-7.
100. Cantaluppi V, Assenzio B, Pasero D, Romanazzi GM, Pacitti A, Lanfranco G, et al. Polymyxin-B hemoperfusion inactivates circulating proapoptotic factors. Intensive Care Med. 2008;34:1638–45. https://doi.org/10.1007/s00134-008-1124-6.
101. Zhang P, Ouyang Q, Zhai T, Sun J, Wu J, Qin F, et al. An inflammation-targeted nanoparticle with bacteria forced release of polymyxin B for pneumonia therapy. Nanoscale. 2022;14:15291–304. https://doi.org/10.1039/D2NR02026B.

Publisher's Note